

# Pre-equilibrium evolution of quark-gluon plasma

Gouranga C Nayak <sup>\*</sup> and V. Ravishankar <sup>†</sup>

*Department of Physics, Indian Institute of technology, Kanpur – 208 016, INDIA*

## Abstract

We study the production and the evolution of quark-gluon plasma expected to be formed in ultra relativistic heavy-ion collisions, within the color flux-tube model. We introduce the gluonic component in the Boltzmann equation, which we solve in the phase space which is extended to include the SU(3) color degree of freedom. The color degree of freedom is shown to play a decisive role in equilibration, and in fixing the temperature of the plasma. We further find that the soft partons that we study here contribute substantially to the bulk properties. Finally, the model is shown to provide a detailed picture of how the quark-gluon plasma evolves and is driven towards a hydrodynamic flow, which starts occurring around  $1\text{ fm}$ .

PACS numbers: 12.38.Mh, 25.75.+r, 0.+y, 12.20.-m, 24.85.+p

Typeset using REVTeX

---

<sup>\*</sup>e-mail:gcn@iitk.ernet.in

<sup>†</sup>e-mail:vravi@iitk.ernet.in

## I. INTRODUCTION

It is by now well established from lattice studies [1] that hadronic matter at sufficiently high temperatures ( $\sim 200\text{MeV}$ ) and pressures undergoes a transition to the so called quark gluon phase involving, i) deconfinement and ii) chiral symmetry restoration, not necessarily simultaneously. It also appears that the deconfinement transition is of the first order, and that the deconfined phase near the critical temperature is still rather far away from showing an ideal gas behaviour. In any case, while such a phase surely did exist in the early universe, it is interesting that we may expect to produce this phase in ultra relativistic heavy ion collisions (URHIC). In fact it is widely believed that RHIC and LHC will succeed in revealing this new phase of matter.

The deconfined phase is not accessible directly in the accelerator experiments. The signatures are therefore necessarily indirect, and the prominent ones that have been studied are : 1)  $J/\psi$  suppression [2], 2) electromagnetic probes such as dilepton and direct photon production [3,4], and 3) strangeness enhancement [5]. However, a proper diagnostics for these signatures in the accelerator produced plasma must involve a study of the evolution of the system in all its stages, including its production soon after the two nuclei have collided with each other, the equilibration, hydrodynamic expansion leading to cooling, and finally hadronization. Note that the above stages are not necessarily mutually exclusive; there could be an overlap between production and equilibration, as also between cooling and hadronization. Of particular importance to us here are the production and the equilibration regimes; indeed it has been pointed out [2,6] that  $J/\psi$  suppression which is generally attributed to the equilibrium stage can also arise from the pre-equilibrium stage, an observation which is true for strangeness enhancement as well. The contribution of the pre-equilibrium stage to the dilepton production and the direct photon production would be even more pronounced, and a careful study of the above signals ought to shed light on this stage of the plasma.

In this paper we discuss the production and the evolution of quark-gluon plasma(QGP) in URHIC by employing the Flux-tube Model [7,8] which is a generalization of the familiar Lund string model widely used for  $e^+e^-$  and  $p-p$  collisions [9]. This model allows for a concurrent production and evolution of quark pairs and gluons by a background chromoelectric field. Assuming the Bjorken scenario [10] where a plateau will be seen in the central rapidity region in relativistic heavy-ion collisions, the Flux-tube model deals with the baryon free plasma in the central region; there would initially be a huge deposit of energy, modeled by the creation of a chromo field between the two receding nuclei, which decays spontaneously to produce partons. Note that the field configuration which contains this energy is necessarily electric like if it has to produce partons. Collisions between the partons and their acceleration (which is again due to the background field) dictate the dynamics of their evolution and equilibration. We propose to study this dynamics within the classical Boltzmann equation, by explicitly incorporating the production in the source term, acceleration by the background chromo-field and also writing down a collision term.

In a recent paper [11] we studied the evolution of a non-abelian  $q\bar{q}$  plasma in the context of color flux-tube model, where it was shown that the non-abelian features have a major role in the evolution of the system in a manner that was not captured in any of the earlier studies [7,8,12] which were purely abelian in their content. It was also argued that it was unlikely that the system would equilibrate instantaneously. However, for simplicity, we had

ignored there the gluonic component and considered the simpler gauge group  $SU(2)$ . In this paper, we remedy both the drawbacks; we consider the gauge group  $SU(3)$  as is appropriate for a real plasma. We also include the gluons, which have been completely ignored so far. We pay attention to the detailed evolution, and its prediction for different bulk properties of the plasma in this paper. Signatures such as dilepton, direct photon and strangeness production from this model will be calculated and reported elsewhere.

There is yet another class of models which describe the evolution of quark-gluon plasma such as heavy-ion jet interaction generator(HIJING) [13] and parton cascade model(PCM) [14]. These models are governed by perturbative QCD (pQCD). The production and the evolution of hard and semi-hard partons are studied by a master rate equation in HIJING and by a transport equation in PCM. While these may be reliable in the study of hard partons, these perturbative approaches are admittedly insufficient to study the dynamics of the soft partons [13], in particular, their production. Being perturbative, they do not incorporate any of the non-perturbative aspects such as the formation of the strings and their break up, which is studied even in  $pp$  collisions. The addition of soft partons to hard and semi-hard partons changes the bulk properties of plasma, such as temperature and energy density. Xu *et al.* [6] have observed that this addition leads to an enhanced suppression of  $J/\psi$ , which can be understood to be a consequence of increased number density and a lowered temperature of QGP. In our study, we employ the Schwinger mechanism [15] for particle production, which is quintessentially non-perturbative. Even if one were to employ a perturbative version, as a time dependent electric field would require [16], it may be noted that an initial electric field as a classical saddle point owes its existence to non-perturbative processes, *viz*, the soft gluon exchanges that take place between the two nuclei. On the whole, one may expect that the pQCD based studies [13,14] will be useful in the hard regime, and that the flux tube like models will be required to study the soft regime which will become increasingly prominent as the system expands and more and more secondaries are produced [17]. Indeed, it should be possible to develop a unified approach to study the hard and the soft components, say *a la* the approach of Eskola and Gyulassy [18] who have included the minijets in their so called chromoviscous hydrodynamics which is again based on the flux tube model. This study will be taken up separately.

The paper is organised as follows. In section **II** we set up the transport equations for the quarks and the gluons in an extended phase space. Section **III** contains a description of the color flux-tube model, and its incorporation into the transport equations. The numerical procedure is presented in section **IV** and the results are discussed and compared with other models in section **V**. We conclude and summarize the main results in section **VI**.

## II. TRANSPORT EQUATION IN EXTENDED PHASE SPACE

In non-abelian theory the color charge is a continuously varying function of time. The precession of the color charge( $Q^a$ ) obeys Wong's equation [19]:

$$\frac{dQ^a}{d\tau} = f^{abc} u_\mu Q^b A^{c\mu} \quad (1)$$

which supplements the Lorentz force equation

$$\frac{dp^\mu}{d\tau} = Q^a F^{a\mu\nu} u_\nu. \quad (2)$$

Here  $A^{a\mu}$  is the gauge potential, and  $f^{abc}$  is the structure constant of the gauge group. In order to include the color charge in the phase-space, we consider an extended one particle phase space of dimension  $d = 6 + (N^2 - 1)$ , (with  $N = 3$ ). The extended phase space is taken to be the direct sum  $R^6 \oplus G$ , where  $G$  is the (compact) space corresponding to the given gauge group. In short, in addition to the usual 6 dimensional phase space of coordinates and momenta we now have another eight coordinates corresponding to the eight color charges in  $SU(3)$ . In this extended phase space a typical transport equation reads as [20]:

$$\left[ p_\mu \partial^\mu + Q^a F_{\mu\nu}^a p^\nu \partial_p^\mu + f^{abc} Q^a A_\mu^b p^\mu \partial_Q^c \right] f(x, p, Q) = C(x, p, Q) + S(x, p, Q) \quad (3)$$

Here  $f(x, p, Q)$  is the single particle distribution function in the extended phase space. The first term in the lhs of equation (3) corresponds to the usual convective flow, the second term is the non-abelian version of the Lorentz force term and the last term corresponds to the precession of the charge as described by Wong's equation.  $S$  and  $C$  on the right hand side of equation (3) correspond to the source and collision terms respectively (described below). Note that we have to write separate equations for quarks, antiquarks and gluons since they belong to different representations of  $SU(3)$ .

The term gluonic source merits some explanation here. The classical background field that we consider here has, in contrast to the Maxwell field, self interaction. We are interested in the stability of the gluonic vacuum (which is the analogue of the radiation in electrodynamics) against the fluctuations in the classical background field. An adaptation of the Schwinger mechanism in QED shows that the fluctuations can indeed produce the gluons, *i.e.* the off-shell classical field can spontaneously produce the on-shell radiative gluonic field (see equation 9). There is, therefore, no ambiguity or double counting in this process. The source term yields asymptotic gluonic states, and further interaction between the gluons is treated separately by a collision term.

### III. THE FLUX-TUBE MODEL

We briefly review the flux tube model as is appropriate to the context here. In this model, the two nuclei that undergo a central collision at very high energies are Lorentz-contracted as thin plates. When these two Lorentz-contracted nuclei pass through each other they acquire a nonzero color charge ( $\langle Q \rangle = 0, \langle Q^2 \rangle \neq 0$ ), by a random exchange of soft gluons. The nuclei which act as color capacitor plates produce a chromo-electric field between them [21,22]. The strength of the field which naturally depends on the strength of the color charge residing on the plates cannot be fixed from first principles. We can only fix that phenomenologically, say by identifying the field energy with the energy in the central region as estimated by Bjorken [10]. This strong electric field creates  $q\bar{q}$  and gluon pairs via the Schwinger mechanism which enforces the instability of the vacuum in the presence of an external field. The partons so produced, collide with each other and also get accelerated by the background field. As described in the previous section, these color charges rotate in the color space, a feature which is manifest in this model, but largely ignored in the earlier

studies [7,8,12]. Thus the production, collision, acceleration and rotation are implemented in one single transport equation, i.e. equation (3).

It is very difficult to solve the transport equation written above, in general. And we have a set of three coupled equations here. As was done in reference [11] we make a few assumptions. First of all, we admit only those potentials which can be brought to a form where the only surviving components are  $A^{\mu a} = (A^{01}, A^{31})$ . This choice restricts  $F^{\mu\nu}$  to be “Maxwell” like, also pointing in the “1” direction in the color space. This restriction is not arbitrary as it is known [23] that the non-Maxwellian configurations - where the charges, the gauge potential and the fields do not lie in the same direction in the group space - do not produce particle pairs, in general. Secondly, we require a boost invariant description of the physical quantities [10]. Accordingly, we demand that the distribution functions also be functions of only boost invariant quantities. Finally, we work within the Lorentz gauge which is implemented elegantly by the choice  $A^{\mu a} = \epsilon^{\mu\nu} \partial_\nu G^a(\tau)$ ,  $\mu, \nu = 0, 3$ , with all the other components zero.  $\tau = (t^2 - z^2)^{1/2}$  is the boost invariant proper time.

Now we fix the magnitude of the vector charge  $Q^a$ , which corresponds to the first Casimir invariant of SU(3). It is simply the value of the coupling constant. There is also another Casimir invariant, *viz*,  $d^{abc} Q^a Q^b Q^c$ , which is also conserved as the QGP evolves. There is, however, no way of fixing its value and the experiments presumably impose no restriction on its allowed values. In fact, the same holds for lattice analyses as well. For this reason, we do not take cognizance of this invariant, and we conveniently resolve the SU(3) charges in the polar coordinates:  $Q_i = Q \prod_{k=1}^{i-1} \sin\theta_k \cos\theta_i$  for  $i \neq 8$ , and  $Q_8 = Q \prod_{k=1}^7 \sin\theta_k$ .

We now fix the collision term. A collision term can be indeed obtained from pQCD. Apart from making the equation hopelessly non-linear, this choice would be good only for the hard components, which are not of interest to us here. As aptly pointed by Hung and Shuryak [24] recently, a microscopic description of collisions gets increasingly cumbersome and also unnecessary as more and more secondaries are produced. On the other hand it is admittedly true that there is no way to reliably obtain a collision term in the non-perturbative regime. So we shall employ a relaxation time approach here, where the relaxation time  $\tau_c$  will have to be fixed phenomenologically, and in all probability, *a posteriori*. Recently it is proposed [25,26] that  $\tau_c$  can be local and have a (weak) dependence on  $\tau$ . We take  $\tau_c$  to be constant here, and further refinements may be incorporated after we have a better understanding of the transport phenomena both experimentally and theoretically.

Within the relaxation time approach, the collision term is written as

$$C = \frac{-p^\mu u_\mu (f - f^{eq})}{\tau_c}. \quad (4)$$

Here  $f^{eq}$  is the distribution function, in local equilibrium. Note that the locality can extend to the color space as well apart from space-time. Taking it to be an ideal gas, for simplicity, we write,

$$f_{q,g}^{eq} = \frac{2}{\exp((p^\mu - Q^a A^{\mu a}) u_\mu / T(\tau)) \pm 1} \quad (5)$$

where the  $+(-)$  sign is to be taken for fermions (bosons). Note that we allow a common equilibrium temperature for quarks and gluons. Here  $u^\mu = (\cosh\eta, 0, 0, \sinh\eta)$  is the flow velocity and  $\eta$  is the space time rapidity given by  $\tanh\eta = z/t$ . With our choice of potentials, it follows that  $A^\mu u_\mu = 0$ , so that the equilibrium distribution function can be written as:

$$f_{q,g}^{eq} = \frac{2}{\exp((p^\mu u_\mu)/T(\tau)) \pm 1} \quad (6)$$

Note also that the temperature depends only on the proper time, in accordance with the Bjorken picture. Demanding the same of the distribution functions as well, we require that the longitudinal boosts be symmetry operations on the single particle distribution. The boost-invariant parameters are, apart from the color charges,

$$\tau = (t^2 - z^2)^{1/2}, \xi = (\eta - y), p_t = (p_0^2 - p_l^2)^{1/2} \quad (7)$$

where  $y = \tanh^{-1}(p_l/p_0)$  is the momentum rapidity.

The above set of invariant variables also serve to express the source terms for  $q\bar{q}$  and gluon pairs which will be obtained by the Schwinger mechanism. The expression for  $q\bar{q}$  production (obtained from constant electric field) is written as [11]

$$S_q(\tau, \xi, p_t, \theta_1) = -\frac{gE \cos \theta_1}{8\pi^3} \ln \left[ 1 - \exp \left( -\frac{2\pi p_t^2}{gE \cos \theta_1} \right) \right] \left( \frac{\alpha}{\pi} \right)^{1/2} \exp(-\alpha \xi^2) \quad (8)$$

and for gluon pair production the corresponding term in SU(3) is given by the relatively stronger term [20,27]

$$S_g(\tau, \xi, p_t, \theta_1) = (3/2)S_q(\tau, \xi, p_t, \theta_1). \quad (9)$$

We put  $g = 4$  throughout our calculation.

Now consider the third term  $f^{abc} A^{\mu a} Q^b \frac{\partial}{\partial Q^c} f(x, p, Q)$ , in the transport equation (3). Due to the restriction of the gauge potentials to the form  $A^{\mu a} = (A^{01}, A^{31})$ , there is an additional simplification in the transport equation. In order to see that, note that equation (3) has the formal solution

$$f_{q,g}(\tau, \xi, p_t, Q) = \int_0^\tau d\tau' \exp\left(\frac{\tau' - \tau}{\tau_c}\right) \left[ \frac{S_{q,g}(\tau', \xi', p_t, Q)}{p_t \cosh \xi'} + \frac{f_{q,g}^{eq}(\tau', \xi', p_t, Q)}{\tau_c} \right], \quad (10)$$

where  $\xi'(\tau')$  is given by

$$\xi' = \sinh^{-1} \left[ \frac{\tau}{\tau'} \sinh \xi + \frac{g \cos \theta_1}{p_t \tau'} \int_{\tau'}^\tau d\tau'' E(\tau'') \right]. \quad (11)$$

Clearly,  $f^{1bc} A^1 Q^b \frac{\partial}{\partial Q^c} f(x, p, Q) = 0$ , as  $S$ ,  $f_{eq}$  and  $\xi'$  only depend on  $Q_1$ .

With this final simplification, we get a set of three equations, one each for quark, anti-quark and gluon respectively. They are, explicitly,

$$\begin{aligned} \left[ \frac{\partial}{\partial \tau} - \left( \frac{\tanh \xi}{\tau} + \frac{g \cos \theta_1 E(\tau)}{p_t \cosh \xi} \right) \frac{\partial}{\partial \xi} \right] f_{q,g}(\tau, \xi, p_t, \theta_1) \\ + \frac{f_{q,g}}{\tau_c} = \frac{f_{q,g}^{eq}}{\tau_c} + \frac{S_{q,g}(\tau, p_t, \xi, \theta_1)}{p_t \cosh \xi} \end{aligned} \quad (12)$$

for quarks and gluons, and

$$\left[ \frac{\partial}{\partial \tau} - \left( \frac{\tanh \xi}{\tau} - \frac{g \cos \theta_1 E(\tau)}{p_t \cosh \xi} \right) \frac{\partial}{\partial \xi} \right] \bar{f}_q(\tau, \xi, p_t, \theta_1) + \frac{\bar{f}_q}{\tau_c} = \frac{f_q^{eq}}{\tau_c} + \frac{S_q(\tau, p_t, \xi, \theta_1)}{p_t \cosh \xi} \quad (13)$$

for antiquarks.

In the process where the field and the particles are present the conservation of energy-momentum is expressed in the form:

$$\partial_\mu T_{mat}^{\mu\nu} + \partial_\mu T_f^{\mu\nu} = 0, \quad (14)$$

where

$$T_{mat}^{\mu\nu} = \int p^\mu p^\nu (2f_q + 2\bar{f}_q + f_g) d\Gamma d\Omega_7, \quad (15)$$

and

$$T_f^{\mu\nu} = \text{diag}(E^2/2, E^2/2, E^2/2, -E^2/2). \quad (16)$$

Here  $d\Gamma = d^3p/(2\pi)^3 p_0 = p_t dp_t d\xi/(2\pi)^2$ , and  $d\Omega_7$  is the angular integral measure in the color space. The factor 2 in the equation (15) is for two flavors of quarks. Now since energy and momentum are conserved in each collision, we have:

$$\int p^\nu C d\Gamma d\Omega_7 = 0. \quad (17)$$

Taking the first moment of the Boltzmann equation, integrating over the color degrees of freedom for  $f_q$ ,  $\bar{f}_q$  and  $f_g$  and making use of equations (14) and (17), we obtain from equation (3)

$$\partial_\mu T_f^{\mu\nu} + gE(\tau) \int d\Gamma d\Omega_7 p^\nu \frac{\partial(2f_q - 2\bar{f}_q + f_g)}{\partial \xi} + 4 \int d\Gamma d\Omega_7 p^\nu S_q + 2 \int d\Gamma d\Omega_7 p^\nu S_g = 0 \quad (18)$$

In the above equation the factor 4 in third term arises because we have two separate transport equations for quark and antiquark, each coming with two flavors, and the factor 2 in fourth term is due to  $gg$  pair production, although there is only one transport equation for gluon. Putting  $\nu = 0$  and 3 in (18) we get two equations, which then yield the following equation for the decay of the electric field:

$$\frac{dE(\tau)}{d\tau} - \frac{2g\gamma}{2\pi} \int_0^\infty dp_t p_t^2 \int_0^\infty d\xi \sinh \xi \int_0^\pi d\theta_1 [2f_q - 2\bar{f}_q + f_g] + (\pi^3/6) \bar{a} |E(\tau)|^{3/2} = 0. \quad (19)$$

Here  $\bar{a} = a\zeta(5/2) \exp(0.25/\alpha)$ ,  $a = c(g/2)^{5/2} \frac{7}{2(2\pi)^3}$  and  $c = \frac{2.876}{(4\pi^3)}$ . Finally,  $\zeta(5/2) = 1.342$  is the Riemann zeta function.

To solve this equation we fix the form of  $T(\tau)$ , by demanding that the particle energy density differ negligibly from the equilibrium energy density, in each collision. We then relate the proper energy density, which is defined by

$$\epsilon(\tau) = \int d\Gamma d\Omega_7 (p^\mu u_\mu)^2 (2f_q + 2\bar{f}_q + f_g), \quad (20)$$

to the temperature by its equilibrium value, whence,

$$T(\tau) = \left[ \frac{10\epsilon(\tau)}{\pi^6} \right]^{1/4}. \quad (21)$$

We solve the equation (19) numerically to see the evolution of quark-gluon plasma.

## IV. NUMERICAL PROCEDURE

The numerical procedure is already discussed in earlier works [11,12]. We use a double self-consistent method. The procedure follows the scheme  $\{T(\tau)_{trial}, E(\tau)_{trial}\} \rightarrow \{f, \bar{f}, E(\tau)\} \rightarrow \{f, \bar{f}\} \rightarrow T(\tau) \rightarrow \dots$  by repeated use of equations (10), (19), (10), (21), which is iterated until there is a convergence to the required degree of accuracy. We have in mind the LHC energies, and we have taken the initial energy density as  $\epsilon_0 = 300 \text{ GeV}/fm^3$ . Compared to PCM [14] where the initial particle energy density is taken to be around  $1300 \text{ GeV}/fm^3$  at RHIC, our choice of initial field energy density might appear some what low. However, our choice is guided by the estimate that the formation time for a qgp is a fraction of a fermi, as we explained in ref [11]. In any case it would not be very appropriate to compare the two initial conditions since the "initiality" is only in a limited sense. Indeed, it is the energy density at the location of the receding color plates, and being well in the fragmentation region at all later times after the collision, what matters is the energy in the central region, corresponding to larger and larger values of  $\tau$  as the system evolves. It will be seen that in this region the results that our study yields are not unreasonable, if we make a judicious choice for the value of  $\tau_c$ . We have studied, in this paper, the results for three different values of  $\tau_c$ . For hydrodynamic and collisionless limits we have choosen  $\tau_c = 0.001 fm$  and  $5.0 fm$ . We have compared the results of these limitng value of  $\tau_c$  to a realistic intermediate value  $\tau_c = 0.2 fm$ .

## V. RESULTS AND DISCUSSIONS

The solution of the transport equations following the procedure outlined in the previous section allows us to determine directly the temporal evolution of the particle and energy densities, temperature and also the rate at which the field energy flows into the particle sector. These quantities are of intrinsic interest and are, in principle, amenable to experimental study via dilepton production. We present these results below. Also of interest are the broader questions: when the equilibration sets in, at what time the flow becomes hydrodynamic - with or without viscous flow [10,27], etc.

Then there are features peculiar to our model. Since the color plates are receding away from each other, energy is continuously pumped into the field, which subsequently decays to produce particles. We study the relative rates at which these two dynamical processes proceed in URHIC. This process cannot of course proceed indefinitely. This has already been observed by Gyulassy and Csernai in their study of the dynamics of fragmentation region [28]. As the plates give up their energy, they decelerate. The deceleration sets limits on the times up to which the model is valid. Indeed, the assumption of boost invariance breaks down as it is strictly exact only if  $v_{plate} = c$ . It is safe to assume boost invariance so long as  $v_{plate} \geq 0.9c$  [29]. A simple estimate shows that this condition, for our choice of initial energy density, holds up to  $\sim 5 - 10 fm$  for LHC energies. There would be other competing processes in the fragmentation region, and the Bjorken scenario is probably valid upto  $3 - 4 fm$ . Keeping this in mind, we have restricted ourselves to (proper) times  $\leq 1.5 fm$ . Note that the results presented below will be applicable for RHIC energies only if  $\tau < 1 fm$ .

Finally, the formulation allows us to study an inherently non-abelian quantity, *viz*,  $\langle \cos^2 \theta \rangle$ , where  $\theta$  is the angle between the charge and the field in the group space. Note



that its abelian counterpart  $\equiv 1$ . Wherever possible, we have compared our results with the earlier  $SU(2)$  study and PCM. We also display the distribution function(s) in the color space, which none of the other models can yield, be they flux tube based or pQCD based. All the results will be shown for the quarks and the gluons separately. We mention here that it is the color Flux-tube model within which one obtains the evolution of the mean background chromoelectric field, which is absent, either in HIJING or PCM. The evolution of such a background field has a greater impact on the acceleration of the partons present in the system, and hence on the observed signatures. For example the  $c\bar{c}$  pair, which is produced in early collisions is acted by this back ground field along with  $c\bar{c}$  potential, to evolve into a physical  $J/\psi$ .

### A. Comparison with $SU(2)$ results

In the earlier work [11] we had argued that the assumption of the so called abelian dominance which was made in a large number of transport studies [7,8,12] does not receive any justification from a proper study of a non-abelian transport equation. The present study reinforces the same idea, as it is only to be expected. In particular, note that a determination of quantities such as the vacuum current or the polarization current [18] will be particularly suspect in view of the fact that the effective charge will only be a fraction of the true charge (see below). There now arises the question of the dependence of the results on  $N$  if one employs the gauge group  $SU(N)$  in solving Equation (3). Although we are not in a position to make a strict comparison between  $SU(2)$  and  $SU(3)$  in this paper because the  $SU(2)$  study had ignored the gluonic terms altogether, it is still useful to see what a limited comparison can yield. We shall restrict ourselves to the value  $\tau_c = 0.2 fm$  to contrast very briefly the results of  $SU(2)$  [11] and  $SU(3)$ .

We shall consider the time dependence of the electric field, the energy density and the number density, shown in Figs. 1-3. First of all, it may be noted that the  $SU(3)$  quantities evolve much more rapidly than their  $SU(2)$  counterparts. In fact, while the number density and the energy density have attained their maximum value around  $1 fm$ , at which time the field also has considerably decayed, there is hardly any activity in the  $SU(2)$  case even upto  $1.5 fm$ . Indeed, at  $\tau \sim 1 fm$ , the number density for  $SU(3)$  is larger by a factor  $\sim 10$ , and the energy, by a factor  $\sim 5$ , even if we consider only the quark sector. Please note that it is not that the energy is merely apportioned between quarks and gluons; the existence of a second channel has in no way decreased the flow to the quark sector.

More significant is the fact that it is the  $SU(3)$  flow that shows the required trend towards a hydrodynamic flow. The  $SU(2)$  counterparts fail to show any such trend all that way upto  $1.5 fm$ . We may certainly expect a hydrodynamic flow to occur at much later times, but in all likelihood it does not seem to happen at any realistic value of  $\tau$ . We shall discuss the  $SU(3)$  flow in more detail in the next section. On the whole, the plasma is denser for  $SU(3)$  due to increased volume in phase space.

## B. Discussion of the results

We now discuss the results for SU(3) in some detail, for three values of  $\tau_c$  - 0.001, 0.2 and 5 fm. The first (last) choice corresponds to the instantaneous hydrodynamic (collisionless) case, in the time scale set by the initial energy density. The quark and the gluonic contributions will be shown separately. It is clear from Figs. 4 and 5 that the quarks and the gluons show the same behaviour regarding the energy density and the number density as functions of proper time. The quark contribution is larger, partly because we have considered two flavors, although the source term [27] favors a larger rate for gluons in the color space. The situation will probably get reversed if we include the more correct perturbative source term for quark [16] and gluon production [30]. In that case, the single and three gluon production rates are of the same order as that of two gluons. That the two sectors will continue to show the same trend may be reliably assumed. The important common feature that Figs. 1, 4 and 5 show is the nature of the evolution at times later than 1 fm. The curves suggest an approach to the hydrodynamic flow. Note that a hydrodynamic flow would imply that  $n(\tau)$ ,  $\epsilon(\tau)$  and  $T(\tau)$  behave like  $\tau^{-1}$ ,  $\tau^{-4/3}$  and  $\tau^{-1/3}$  respectively. We find that the corresponding exponents are  $-0.7$ ,  $-1.23$  and  $-0.31$  respectively. While the temperature scaling suggests a close approach to the free flow regime, the other two exponents show the presence of drag [32], implying that collisions have not completely ceased. It may be expected that full hydrodynamic flow will take over around 2 fm.

First of all let us compare the results for quarks and gluons separately, for  $\tau_c = 0.2$  fm before presenting the results for different values of  $\tau_c$ . In fig-4 we have presented the scaled particle energy densities. In contrast to HIJING and PCM, we obtain lower values for energy and number densities for gluons than that of quarks and antiquarks together (fig-5). For a complete study, a source term for hard parton production is also required and this term can be obtained from minijet production at these collider energies, following say ref [18]. The importance of the non-perturbative contribution may be gauged qualitatively by noting that the peak number density for quark-antiquark together (for two flavors) in this model is  $\simeq 60 / fm^3$  in contrast to the PCM value of  $\simeq 120 / fm^3$  (for three massless flavors). The energy density for quark sectors in PCM is also larger by the same factor, implying that the average energy per particle is of the same order in both the cases.

Let us now consider  $\langle \cos^2\theta \rangle$  (where  $\theta$  is the angle between color charge and the chromoelectric field in color space). This quantity is a good bench mark to characterise the ‘non-abelian’ness of the system, and we present our results in fig-6. This quantity is gauge invariant and physical. It may be seen that this value saturates at  $\theta \simeq \pi/4$ , for both quarks and gluons. This value was always unity in an abelian plasma, as  $\theta \equiv 0$  in that case.

This has a direct impact on the equilibration of the plasma. The equilibration is faster around  $\theta \simeq \pi/2$  where the background field effect is zero, and is slower at  $\theta \simeq 0$ . This is understood as follows. At larger value of  $\theta$ , say around  $\pi/2$ , there is no acceleration of partons by the background electric field. Only collisions are present at this angle, and hence the rate of equilibration is faster. On the otherhand when the angle  $\theta = 0$ , the acceleration of partons by background field retards the equilibration of the partons. At any intermediate values of  $\theta$ , the rate of equilibration lies in between these two extreme values. So this average value, which is purely due to the non-abelian nature of the theory, has a major role in the equilibration of the plasma. This is more clearly shown in the distribution functions which

carry the color degrees of freedom explicitly (see fig-7 and fig-8).

We conclude the discussion at  $\tau_c = 0.2 fm$  by making an interesting observation. As can be seen in fig-6, the value of  $\langle \cos^2\theta \rangle$  fluctuates around its mean value for both quarks and gluons, with similar fluctuations in other quantities as well - although it is not that pronounced in them. While it certainly indicates that the distribution is approaching its equilibrium value asymptotically, the question is whether the fluctuations would persist even as the system hadronises. Unfortunately, it is difficult to make any definite assertion at this stage. Indeed, as pointed earlier, evolution of the system beyond  $3 - 4 fm$  requires a full treatment beyond the assumption of the Bjorken scenario in the central region. It is also not known when the hadronization exactly sets in. However, if one assumes that the fluctuations do indeed persist, it may quite well happen that it will manifest as an anisotropy in the parton momentum distribution. This has been pointed out in a study of the related ‘color filamentation’ by Mrowczynski [31]. It is also possible [34], although we do not know in what manner, that these fluctuations in the hadronic phase show up as disoriented chiral condensates. It is only a more complete and rigorous study that can settle the status of these speculations.

Now we present the data for the other two values of  $\tau_c$ , namely  $\tau_c = 0.001 fm$  and  $\tau_c = 5 fm$ , corresponding to hydrodynamic and collisionless limits respectively. These results are then compared with  $\tau_c = 0.2 fm$ . Consider first the number density  $n(\tau)$ . This quantity is seen to be sensitive to the values of  $\tau_c$ . As can be seen from fig-9,  $n(\tau)$  is larger in the hydrodynamic limit, where the maximum value is around 120 per  $fm^3$ , at  $\tau \simeq 1.0 fm$ . As  $\tau_c$  is increased to  $0.2 fm$  we find a lesser value, the maximum value being around  $80/fm^3$ . This trend continues for collisionless limit where particle density is still less. The increase in number density as  $\tau_c$  is decreased is expected in the context of classical theory. This is because, the collision time in any classical non-equilibrium theory depends roughly on the inverse of the number density, apart from the other factors. The behaviour of number densities in fig-9 for different values of  $\tau_c$  in our calculation also reflects the above fact.

In fig-10 we present the scaled energy densities for different values of  $\tau_c$ . Unlike the number density, there is no strong dependence on  $\tau_c$ . This means that the average energy per particle is different for different values of  $\tau_c$ . We find that for  $\tau_c = 0.001 fm$ , the maximum average energy per particle is around 1.0 GeV, whereas it is around 2.0 GeV for  $\tau_c = 0.2 fm$  and 4.0 GeV for  $\tau_c = 5.0 fm$ . Note that these high energy deconfined partons can produce secondary partons, such as strange quarks and also can break a fully formed  $J/\psi$  as analysed by short-distance QCD in reference [33].

Let us consider the electric field. It may be seen from fig-11 that the decay of the field is very slow at  $\tau_c = 0.001 fm$ , compared to  $\tau_c = 0.2$  and  $5 fm$ . Only 30 percent of the field has decayed in the hydrodynamic limit in comparison to collisionless and intermediate limits, where the decay is very large. At the other end in the collisionless limit, the decay is at a slightly slower rate in comparison to  $\tau_c = 0.2 fm$ , implying that the maximal conversion rate is for  $\tau_c$  around  $0.2 fm$ . As mentioned earlier, one peculiarity of the model is that the field energy is continuously created due to the recession of the plates even as the field itself decays to produce particles. To study this, in fig-12 we present field energy per unit transverse area as a function of *ordinary* time. For  $\tau_c = 0.2 fm$  this energy is much less than that at  $\tau_c = 5 fm$  and  $0.001 fm$ . This demonstrates that the conversion is indeed dominant at  $\tau_c = 0.2 fm$ . This is more clearly displayed in fig-13, where we have plotted the ratio of

particle energy per unit transverse area to field energy per unit transverse area.

In fig-14 we present the evolution of temperature at  $\tau_c = 0.2 fm$ . The maximum temperature we obtain in the color flux-tube model is around 300 MeV. Finally, a brief comment on the distribution functions for quarks and gluons with explicit color dependence (see fig-7 and 8). As discussed earlier, it may be seen that the equilibration is fastest for  $\theta = \pi/2$ , where there is no background effect. At  $\theta = \pi/2$  the thermal equilibration occurs at a common time  $\tau \simeq 1.0 fm$  for both quarks and gluons.

## VI. CONCLUSION

We have studied the production and the equilibration of a genuinely non-Abelian plasma with the color degree of freedom incorporated in both the source term and the background term in the transport equation. With the realistic gauge group SU(3) that we have considered here, the distribution functions for quarks and gluons get defined in the extended phase space of dimension 14. We have added the gluonic component into the color flux-tube model, which was so far absent.

The role of the color degree and that of gluons was found to be substantial, and non-trivial. The plasma is denser than the SU(2) counter part but is comparable to the Abelian case. However, it is much cooler than the abelian plasma, where the corresponding temperature is  $\sim 800 MeV$ . The value of the effective charge is larger than that of its counterpart in SU(2), contrary to naive expectations. The peak energy per particle is  $\simeq 2 GeV$  which indeed is the demarcating scale [13] between soft and hard processes. In short, the non-perturbative aspects of the evolution of QGP offer a rich variety of results which will have to be combined with the perturbative studies in order to obtain a complete description of the production and evolution of quark-gluon plasma.

## REFERENCES

- [1] F. Karsch and E. Laermann, Rep. Prog. Phys. **56**, 1347 (1993); Y. Iwasaki *et al.*, Phys. Rev. Lett. **67**, 3343 (1991); F. R. Brown *et al.*, *ibid* **65**, 2491 (1990).
- [2] T. Matsui and H. Satz, Phys. Lett. B **178**, 416 (1986).
- [3] M. T. Strickland, Phys. Lett. B **331**, 245 (1994).
- [4] Jan-e Alam, Sibaji Raha and Bikash Sinha, Phys. Rep. **273** 243 (1996).
- [5] J. Rafelski and B. Muller, Phys. Rev. Lett. **48**, 1066 (1982), C. P. Singh, phys. Rev. Lett. **56**, 870 (1990).
- [6] Xiao-Ming Xu *et al.*, Phys. Rev. C **53**, 3051 (1996).
- [7] G. Baym, Phys. Lett. **138B**, 18 (1984)
- [8] K. Kajantie and T. Matsui, Phys. Lett. **164B**, 373 (1985).
- [9] B. Andersson *et al.* Phys. Rep. **97**, 31 (1983), Nucl. Phys. B **281**, 289 (1987).
- [10] J. D. Bjorken, Phys. Rev D **27**, 140 (1983)
- [11] G. C. Nayak and V. Ravishankar, Phys. Rev. D **55**, 6877 (1997)
- [12] B. Banerjee, R. S. Bhalerao and V. Ravishankar, Phys. Lett. B **224** 16 (1989)
- [13] X. N. Wang, Phys. Rep. **280**, 287 (1997).
- [14] K. Geiger, Phys. Rep. **258**, 237 (1995).
- [15] J. Schwinger, Phys. Rev. **82**, 664 (1951)
- [16] R. S. Bhalerao and V. Ravishankar, Phys. Lett B **409**, 38 (1997).
- [17] K. J. Eskola, B. Muller and X. N. Wang, Phys. Lett. B **374**, 20 (1996).
- [18] K. J. Eskola and M. Gyulassy, Phys. Rev. C **47**, 2329 (1993).
- [19] S. K. Wong, Nuovo Cemento A **65**, 689 (1970)
- [20] H-T Elze and U. Heinz, Phys. Rep. **183** 81 (1989)
- [21] F. E. Low, Phys. Rev. D **12** 163 (1975)
- [22] S. Nussinov, Phys. Rev. Lett. **34**, 1286 (1975).
- [23] L. S. Brown and W. I. Weisberger, Nucl. Phys B. **157**, 285 (1979).
- [24] C. M. Hung and E.V. Shuryak, report no hep-ph/9709264
- [25] S. M. H. Wong, **LP THE-orsay** 96/07.
- [26] H. Heiselberg and X. N. Wang, Phys. Rev. C **53**, 1892 (1996).
- [27] M. Gyulassy and A. Iwazaki, Phys. Lett. B **165B**, 157 (1985).
- [28] M. Gyulassy and L. P. Csernai, Nucl. Phys. A **460** 723 (1986).
- [29] Increasing the accuracy by another 5 percent does not substantially alter the estimate.
- [30] G. C. Nayak and V. Ravishankar, in preparation.
- [31] Stanislaw Mrowczynski, Phys. Lett. B **393** 26 (1997).
- [32] see ref [18]. The Ohmic heating in the reference is realised by the particle production in our model.
- [33] D. Kharzeev and H. Satz, *in Quark-Gluon plasma II, edited by* R. C Hwa (World Scientific, Singapore, 1995), p. 395.
- [34] see, e.g., K. Rajagopal, CALT-68-2104, who has discussed the possible impact of non-equilibrium state on the formation of disoriented chiral condensates.

### Figure captions

**FIG. 1.** Decay of the chromoelectric field as a function of proper time (in units of fermi), for  $\tau_c = .2fm$ . The solid line refers to SU(3) case, and the dashed line to SU(2) case.

**FIG. 2.** The particle energy density scaled w.r.t the initial field energy density as a function of proper time (in units of fermi), for  $\tau_c = .2fm$ . The solid line refers to SU(3) case, and the dashed line to SU(2) case.

**FIG. 3.** The particle number density as a function of proper time (in units of fermi), for  $\tau_c = .2fm$ . The solid line refers to SU(3) case, and the dashed line to SU(2) case.

**FIG. 4.** The particle energy density scaled w.r.t the initial field energy density as a function of proper time (in units of fermi), for  $\tau_c = .2fm$ . The solid line refers to total energy density, upper dashed line to quark plus antiquark energy density, and lower dashed line to the gluon energy density.

**FIG. 5.** The particle number density as a function of proper time (in units of fermi), for  $\tau_c = .2fm$ . The solid line refers to total number density, upper dashed line to quark plus antiquark number density, and lower dashed line to the gluon number density.

**FIG. 6.**  $\langle \cos^2\theta \rangle$  as a function of proper time (in fermi) at  $\tau_c = .2fm$  for quark (solid line) and gluon (dashed line)

**FIG. 7.**  $f_q/f_q^{eq}$  as a function of proper time at  $p_t = 300MeV$ ,  $\xi = 0$  and  $\tau_c = 0.2fm$ , for different values of  $\theta$ . Solid line corresponds to  $\theta = \pi/2$ .

**FIG. 8.**  $f_g/f_g^{eq}$  as a function of proper time at  $p_t = 300MeV$ ,  $\xi = 0$  and  $\tau_c = 0.2fm$ , for different values of  $\theta$ . Solid line corresponds to  $\theta = \pi/2$ .

**FIG. 9.** The particle number density as a function of proper time (in units of fermi), for  $\tau_c = .2fm$  (solid line), for  $\tau_c = 0.001fm$  (upper dashed line) and for  $\tau_c = 5fm$  (lower dashed line).

**FIG. 10.** The particle energy density scaled w.r.t the initial field energy density as a function of proper time (in units of fermi), for  $\tau_c = .2fm$  (solid line), for  $\tau_c = 0.001fm$  (upper dashed line) and for  $\tau_c = 5fm$  (lower dashed line).

**FIG. 11.** Decay of the chromoelectric field as a function of proper time (in units of fermi), for  $\tau_c = .2fm$  (solid line), for  $\tau_c = .001fm$  (upper dashed line) and for  $\tau_c = 5fm$  (lower dashed line).

**FIG. 12.** The field energy/unit transverse area(in units of  $GeV/fm^2$ ) for  $\tau_c = 0.2 fm$  (solid line), for  $\tau_c = 0.001 fm$  (upper dashed line) and for  $\tau_c = 5 fm$  (lower dashed line), as a function of ordinary time (in fermi).

**FIG. 13.** The ratio of particle energy per unit transverse area to field energy per unit transverse area for  $\tau_c = 0.2 fm$  (solid line), for  $\tau_c = 5 fm$  (upper dashed line) and for  $\tau_c = .001 fm$  (lower dashed line), as a function of ordinary time (in fermi).

**FIG. 14.** Evolution of temperature as a function of proper time (in fermi), for  $\tau_c = 0.2 fm$ .

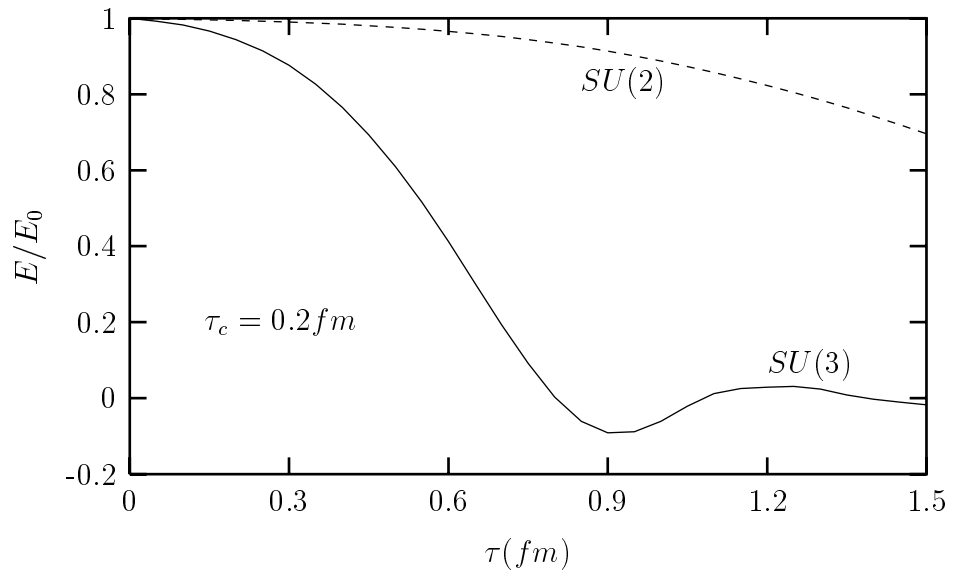


*Fig – 1*

NAYAK AND RAVISHANKAR

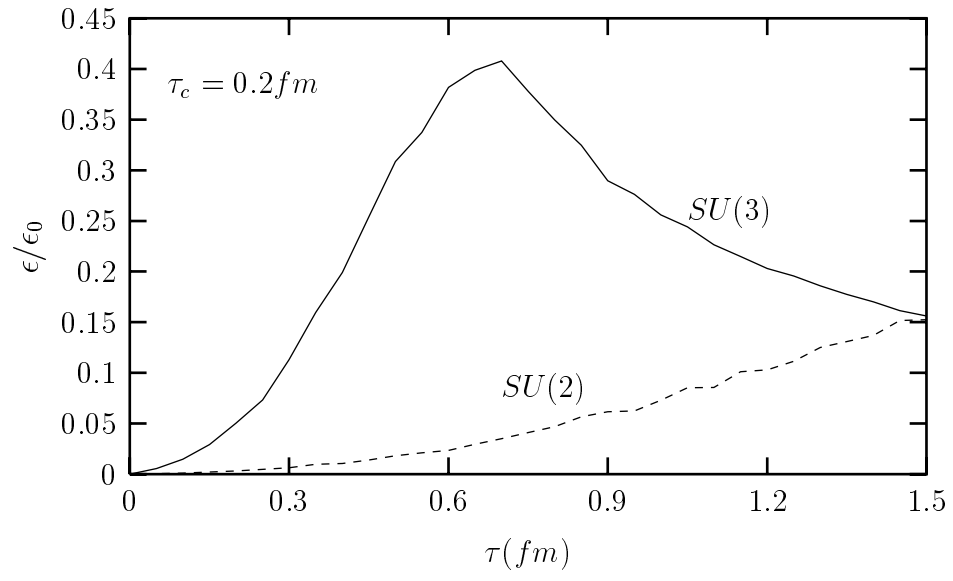


*Fig – 2*

NAYAK AND RAVISHANKAR



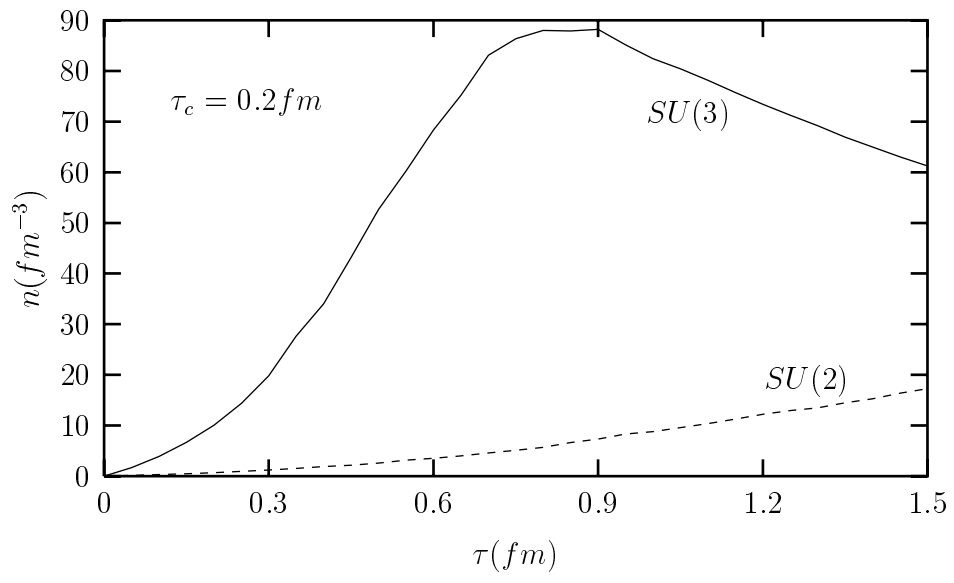


*Fig – 3*

NAYAK AND RAVISHANKAR

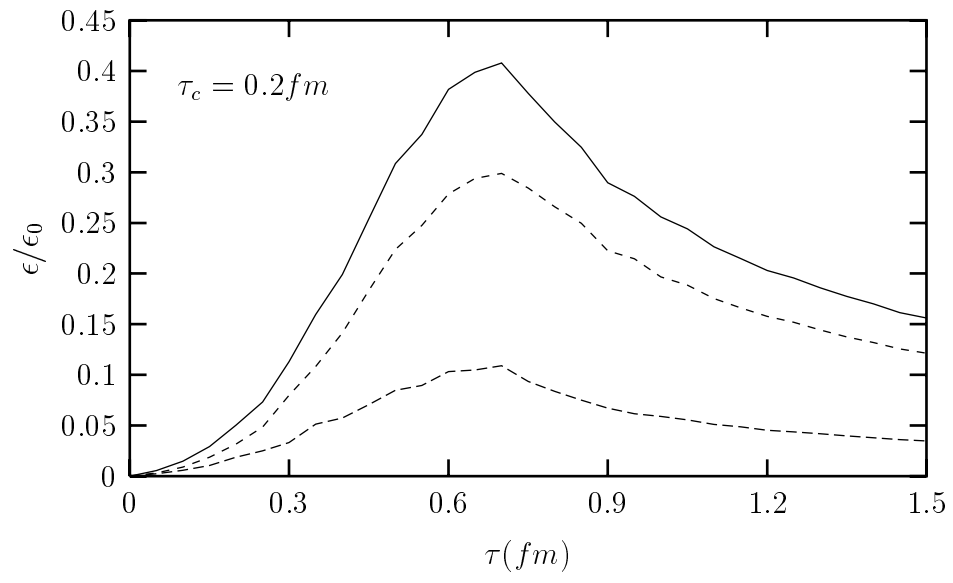


*Fig - 4*

NAYAK AND RAVISHANKAR

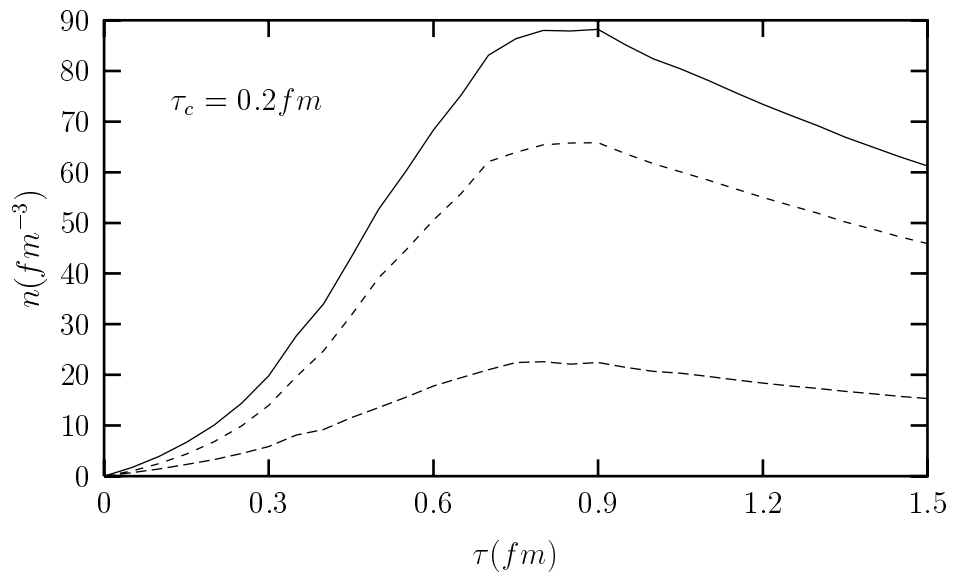


*Fig – 5*

NAYAK AND RAVISHANKAR

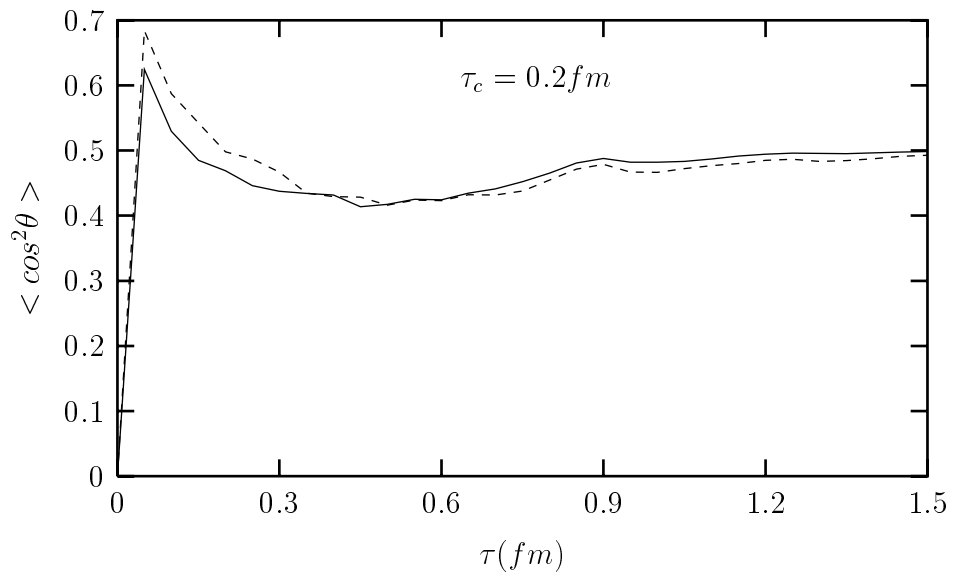


*Fig - 6*

NAYAK AND RAVISHANKAR

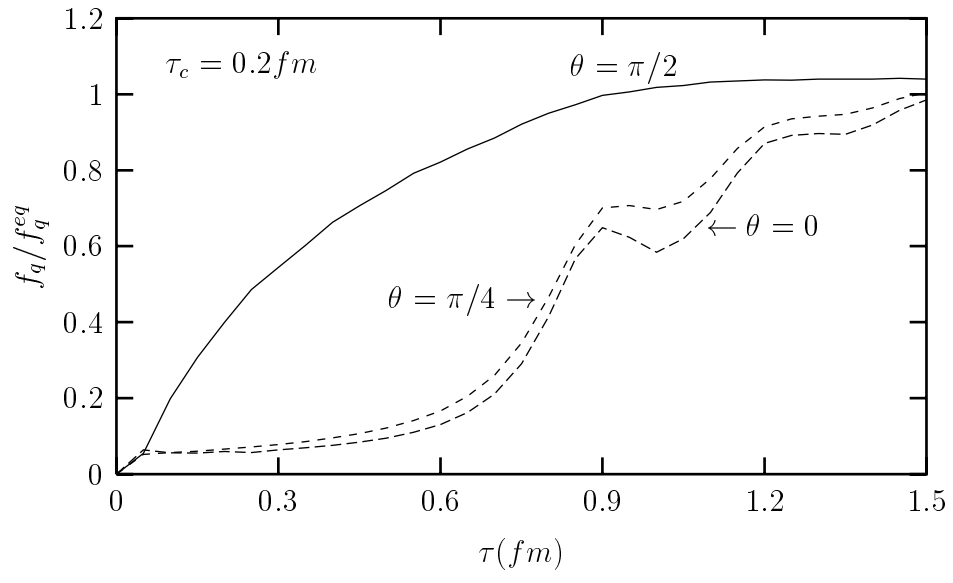


Fig - 7

NAYAK AND RAVISHANKAR

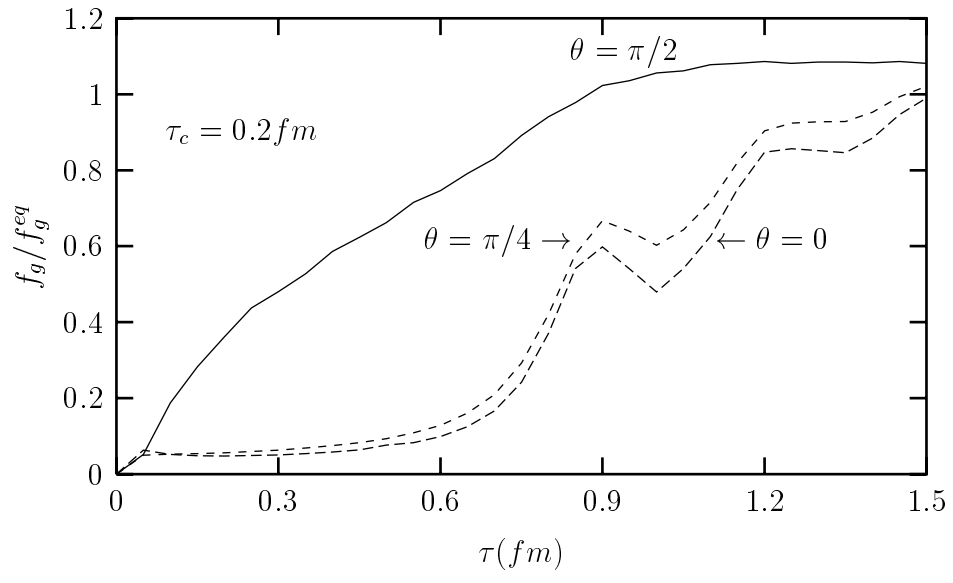
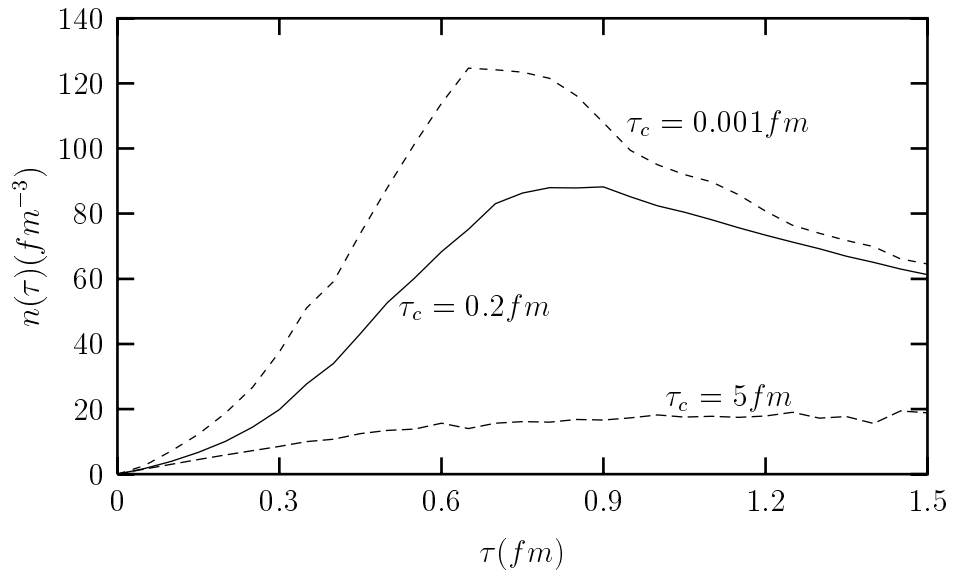


Fig - 8

NAYAK AND RAVISHANKAR



*Fig - 9*

NAYAK AND RAVISHANKAR

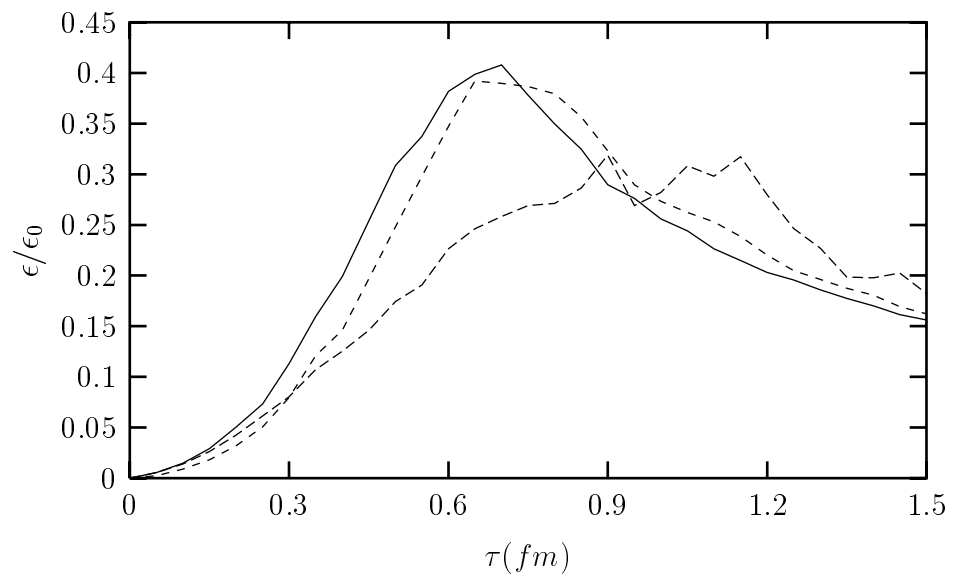


*Fig – 10*

NAYAK AND RAVISHANKAR



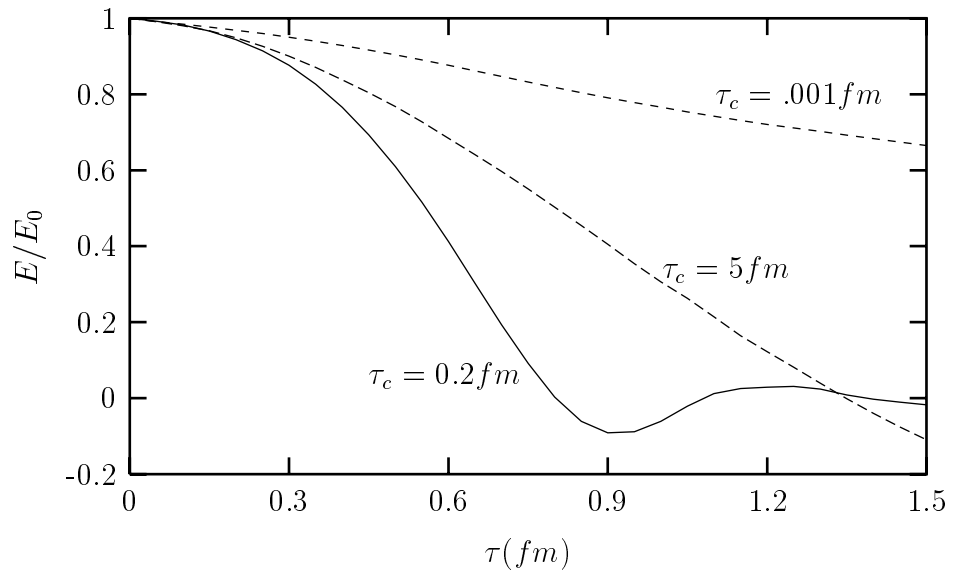


*Fig - 11*

NAYAK AND RAVISHANKAR

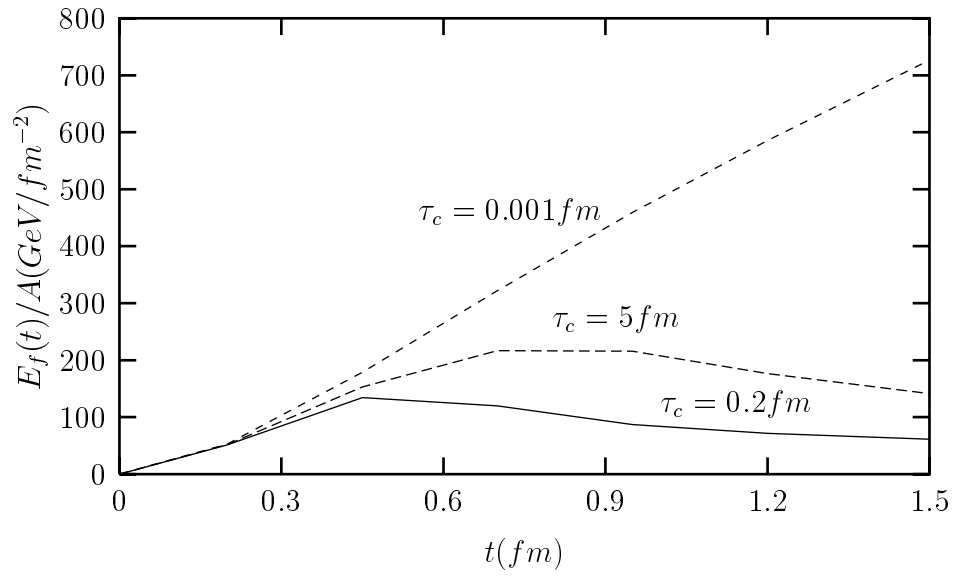


*Fig - 12*

NAYAK AND RAVISHANKAR

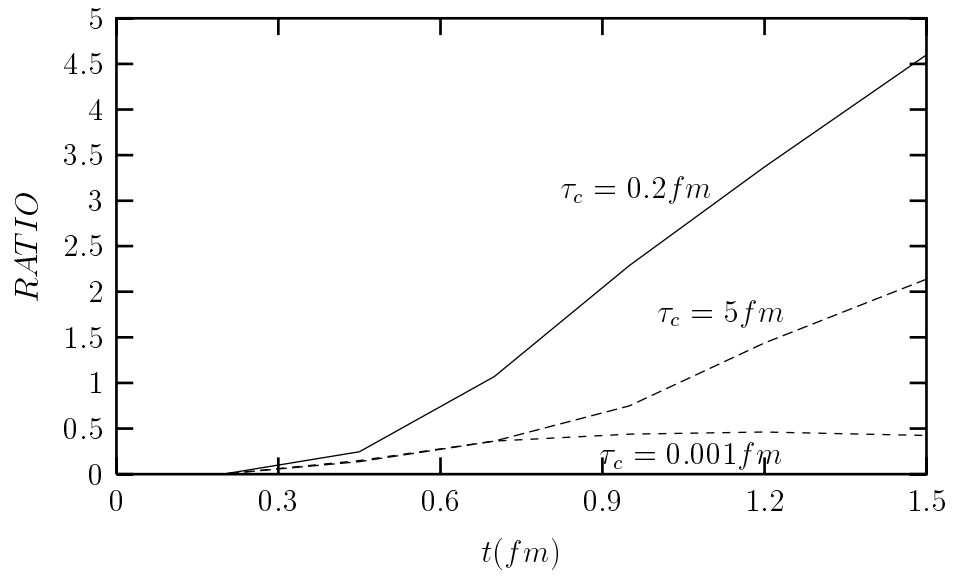


*Fig – 13*

NAYAK AND RAVISHANKAR

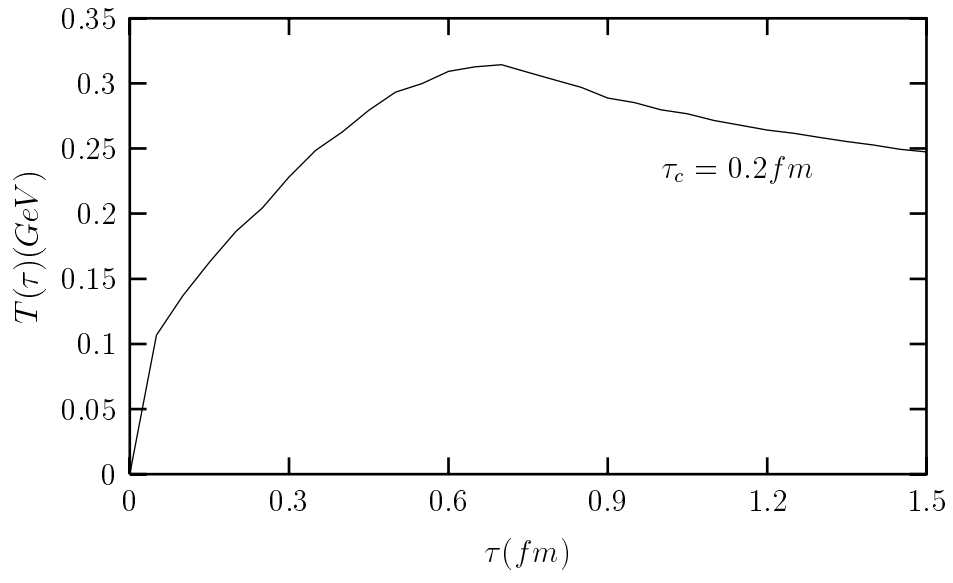


*Fig – 14*

NAYAK AND RAVISHANKAR